nature communications

Article

https://doi.org/10.1038/s41467-024-55604-0

Delivery of Prime editing in human stem cells using pseudoviral NanoScribes particles

Received: 11 June 2024

Accepted: 17 December 2024

Published online: 04 January 2025

Check for updates

Thibaut Halegua[1], Valérie Risson[2], Julien Carras[2,3], Martin Rouyer[1], Laurent Coudert[2], Arnaud Jacquier[2,3,4], Laurent Schaeffer[2,3,4], Théophile Ohlmann[1] ✉ & Philippe Emmanuel Mangeot[1] ✉

Prime Editing can rewrite genes in living cells by allowing point mutations, deletions, or insertion of small DNA sequences with high precision. However, its safe and efficient delivery into human stem cells remains a technical challenge. In this report, we engineer Nanoscribes, virus-like particles that encapsidate ribonucleoprotein complexes of the Prime Editing system and allow their delivery into recipient cells. We identify key features that unlock the potential of Nanoscribes, including the use of multiple fusogens, the improvement of pegRNAs structures, their encoding by a Pol II system and the optimization of Prime-Editors. Nanoscribes edit HEK293T with an efficiency of 68% at the *HEK3* locus with increased fidelity over DNA-transfection and support pegRNA-multiplexing. Importantly, Nanoscribes permit editing of myoblasts, hiPSCs and hiPSCs-derived hematopoietic stem cells with an editing efficiency up to 25%. Nanoscribes is an asset for development of next generation genome editing approaches using VLPs.

Amongst recent gene editing techniques, Prime Editing (PE) stands out for its ability to precisely rewrite genes in living cells by allowing nucleotide substitutions, deletions or insertion of small DNA sequences without induction of double strand DNA breaks[1]. PE does not rely on DNA donor template, is associated with very little cellular toxicity, virtually no indel formation, off-target editing, or by-stander mutations[1–5]. As such, it appears as the ideal tool for editing genetic sequences in pathological contexts. It is especially well-suited for treating human diseases that can be addressed through minor DNA changes. Moreover, it holds promises for conditions lacking current therapies, such as diseases involving dominant triplet repeat alleles, which can be addressed by Single nucleotide variant alterations[6].

PE involves the concerted action of a prime editing guide RNA (pegRNA) and a Cas9-nickase H840A protein fused to a reverse transcriptase domain (RT). Once targeted to a specific locus, the nickase cleaves the target DNA to allow hybridization of the Primer Binding Site (PBS) of the pegRNA where which used as template for reverse transcription. This process results in the generation of a new reverse-transcribed DNA strand, which can be permanently integrated into the edited cell genome after acceptance by DNA reparation-mechanisms and MMR[2].

These unique features make PE one of the most promising tool to perform genome editing with accuracy, safety and limited side effects. Nonetheless, despite this potential, reports on successful use for ex vivo genome editing of fragile cells such as HSCs or hiPSCs remains challenging, mostly due to the lack of efficient and harmless delivery system in these cells.

As such, non-viral delivery methods in the form of mRNAs or RiboNucleoProteins (RNPs) have been developed and successfully used both in cells and in vivo[2,5,7,8]. However, the size of the effector PE protein (about 240 kDa) associated with the technical challenge to synthesize complex epegRNAs in-vitro limit a wider use of this approach[9].

Accordingly, viral delivery methods have been proposed by several groups using lentivirus[10], adenoviruses and adeno-associated viruses (AAVs). Due to their low immunogenicity and broad tropism,

[1]CIRI, Centre International de Recherche en Infectiologie Univ Lyon, Inserm, U1111, Université Claude Bernard Lyon 1, CNRS, UMR5308, ENS de Lyon, F-69007 Lyon, France. [2]Pathophysiology and Genetics of Neuron and Muscle, CNRS UMR 5261, INSERM U1315, Université Lyon1, Faculté de Médecine Lyon Est, F-69008 Lyon, France. [3]Hospices Civils de Lyon, groupement Est, F-69, Bron, France. [4]These authors contributed equally: Arnaud Jacquier, Laurent Schaeffer. ✉e-mail: theophile.ohlmann@inserm.fr; philippe.mangeot@inserm.fr

AAVs are good candidates but they have a limited cargo size of about 4.7 kb in length, which is not sufficient to host prime editor and pegRNA[11]. This has been partially resolved by splitting the AAV system[12] and using optimized versions of effectors. These elaborated approaches recently achieved efficient editing results in animals[13,14]. Unlike AAVs, adenoviruses exhibit a larger packing capacity (8.5 kb) to pack the prime editor system in a single particle and were used with success in the mouse liver and mammalian cells[13]. However, adenovirus trigger a strong inflammatory response in vivo which restricts their use for clinical assays[15]. Moreover, AAVs can integrate in the genome and generate episomes via ITR-mediated recombination that can persist and interfere with the host genome[16].

Virus-like particles (VLPs) derived from retroviral or lentiviral precursors offer an attractive, validated alternative for the transfer of genome-engineering factors[17–19]. Relatively easy to produce, they can incorporate proteins, mRNAs, and be pseudotyped with various envelopes that can modulate their affinity for specific targets[20–23] or increase their stability[24,25]. Moreover, VLP-delivery avoids the sustained expression of nucleases and nickases and reduces the risk of off-targets and indels[26,27] and the induction of the p53-dependent apoptotic pathway[28]. Although the encapsidation limit of GAG-VLPs remains to be documented, they can accommodate and deliver RNA-loaded proteins up to 286 KDa[29], and therefore appear adapted for the packaging of PE-RNPs.

Expanding on our prior findings[29], we develop a PE-VLP system named Nanoscribes optimized both at the level of the Prime-Editor, and the architecture of the particle. As a result, Nanoscribes attain a level of efficiency in gene editing that was comparable to DNA transfection of PE components. In addition, Nanoscribes exhibit a higher fidelity on their target as compared with transfection, they allow multiplex gene editing and are capable of successfully transducing primary cells, hiPSCs as well as their derivative progenitors such as hematopoietic stem cells (HSCs).

Results

We first developed a HEK293T reporter-cell line (named SWYS) with a stably integrated YFP cassette harboring a premature stop codon (YFPs) (Supplementary Fig. 1a). The PE2 system was transfected in SWYS cells together with 5 pegRNAs bearing PBS of different lengths designed to suppress the premature stop codon (Supplementary. Fig. 1b, left). Results showed that a 13-nucleotides long PBS was the optimal size for rescue with over 70% of YFPs conversion (Supplementary Fig. 1b, right). Further verification that YFP expression was maintained after several passages of the cells validated the SWYS cell lines as a tool to measure PE efficiency.

Optimizing the PE-VLPs

Based on the architecture of our previous Cas9-VLP system, we have generated constructs coding for GAG-Cas9n-RT (GAG-PE V1), GAG-POL (Helper) and pegRNA together with a set of 3 fusogens (VSV-G, BAEV, Syncitin-1) (Fig. 1a, left). Expression of these plasmids in HEK293T producer cells generated the first generation of PE-VLPs which can edit SWYS cells at about 1% (Fig. 1b, right) which is extremely low compared to the 70% obtained with DNA transfection (Supplementary Fig. 1b). This prompted us to improve the design of the VLP-PE system.

We have first modified the GAG-PE V1 construct by deleting the RNase-H domain of the RT (ΔR) and/or inserting 3 Nuclear Export Signals of HIV-1 (3n) flanked by 2 protease cleavage sites (P) to give rise to GAG-PE V2, V3 and V4 (Fig. 1b left). Transduction of the SWYS cells by PE-VLPs (V1 to V4) showed that these modifications improved by 3- to 8-fold the efficiency of V1 to reach a maximum of 7% of editing with V4 (ΔR and 3nP) (Fig. 1b, right).

The pegRNA plays an essential role and previous work has shown that 3′ addition of the trimmed EvoPreQ1 pseudoknot (epegRNA) significantly improved the efficacy of PE[5]. Accordingly, we confirmed these data (Fig. 1c right, compare pegRNA and epegRNA) and we reasoned that other stable RNA structures could further strengthen this effect. Thus, we have inserted either the MS2 stem loop[30], or the PP7 stem loop[31] or a motif derived from the TAR structure from HIV-1[32] upstream to the trimmed EvoPreQ1 motif (Fig. 1c). epegMRNA, epegPRNA and epegTRNA were packaged into VLPs and used to transduce SWYS cells and significantly increased editing efficiency compared to the pegRNA and the epegRNA with a maximum editing efficiency of 47% with the ePegTRNA.

It is noteworthy that the use of the epegTRNA also improved PE efficiency from plasmid transfection but only with a moderate editing increase of 1.2-fold (Supplementary Fig. 1c). This enhancement was validated in the A549 and U2OS cell lines by transduction (Supplementary Fig. 1d).

We then sought to compare the accuracy of the editing process between PE-VLPs and PE delivered by DNA transfection. To address this question, we designed a ‘target mismatch-tolerance assays’ in which one, or two mismatches, were introduced into the YFPs cassette, compromising the perfect hybridization of the epegTRNA both at the level of the crRNA and the PBS (Fig. 1d). Transfection with plasmids encoding PE2 (Fig. 1e, orange bars) or transduction with PE-VLPs (V4) (blue bars) achieved editing efficiency of 70% and 50%, respectively. These were normalized to 100 % in each condition to evaluate the impact of mismatches independently of biases arising from variation in overall editing efficiency. When one mismatch was introduced (Fig. 1e), we still measured 8% of YFP-conversion into the transfected cells, whereas PE-VLPs transduction led to a barely detectable level of editing. With two mismatches, the score dropped down to 0,25% for transfected cells and remained barely detectable for transduction (Fig. 1e, bottom panel). This result highlights the accuracy of the PE-VLP transduction method compared with plasmid transfection which retains a significant level of imprecision.

Throughout this study, significant advancements were made in the components of PE, including the development of an optimized Cas9n-RT fusion protein, termed PEmax[2]. Based on these, we engineered a series of GAG-PEmax constructs (V5-V12) that incorporate the improved features previously described (Fig. 2a). Briefly, all the even-numbered constructs carry the RNAseH deletion (V6, V8, V10 and V12). The 3xNES motif (3n) was added on the V7 to V12 constructs at the very C-terminus of the GAG-PEmax fusion (V7-V8), between GAG and PEmax (V9-V10) or duplicated at both positions (V11-V12). One to three proteolytic cleavages sites (P) were added either next to the 3xNES or flanking the 3xNES signal as indicated on the figure. These plasmids were used in producer cells to generate VLPs for the transduction of SWYS cells (Fig. 2b), demonstrating that the V7 construct was the most effective in editing YFP, achieving an efficiency of 63%. Lastly, we show that the efficacy of editing evolved within a linear range with the concentration of PE-VLPs delivered to SWYS cells until it reaches a plateau indicating the maximal editing abilities (Supplementary Fig. 1e).

We next evaluated the PE-VLPs (V4) in the context of human endogenous genes by targeting the *HEK3* and *RNF2* human loci in HEK293T cells. Genotyping of transduced cells revealed editing efficiencies of 31% for the strategy inserting a CTT-triplet in the *HEK3* locus and close to 7.5% for the 1–5 deletion, while editing was barely detectable for the *RNF2* gene (Fig. 2c).

Broadening the capacity of PE-VLPs by the use of a Pol II promoter

The relative low editing efficiency, particularly at the endogenous *RNF2* locus prompted us to further optimize the performance of PE-VLPs. The expression of epegRNAs is regulated by a U6/Pol III promoter which may limit the tool’s applicability due to potential inhibition by a stretch of four consecutive thymines. This is an issue since data from the Clinvar Database show that about 11% (out of 93561

https://doi.org/10.1038/s41467-024-55604-0

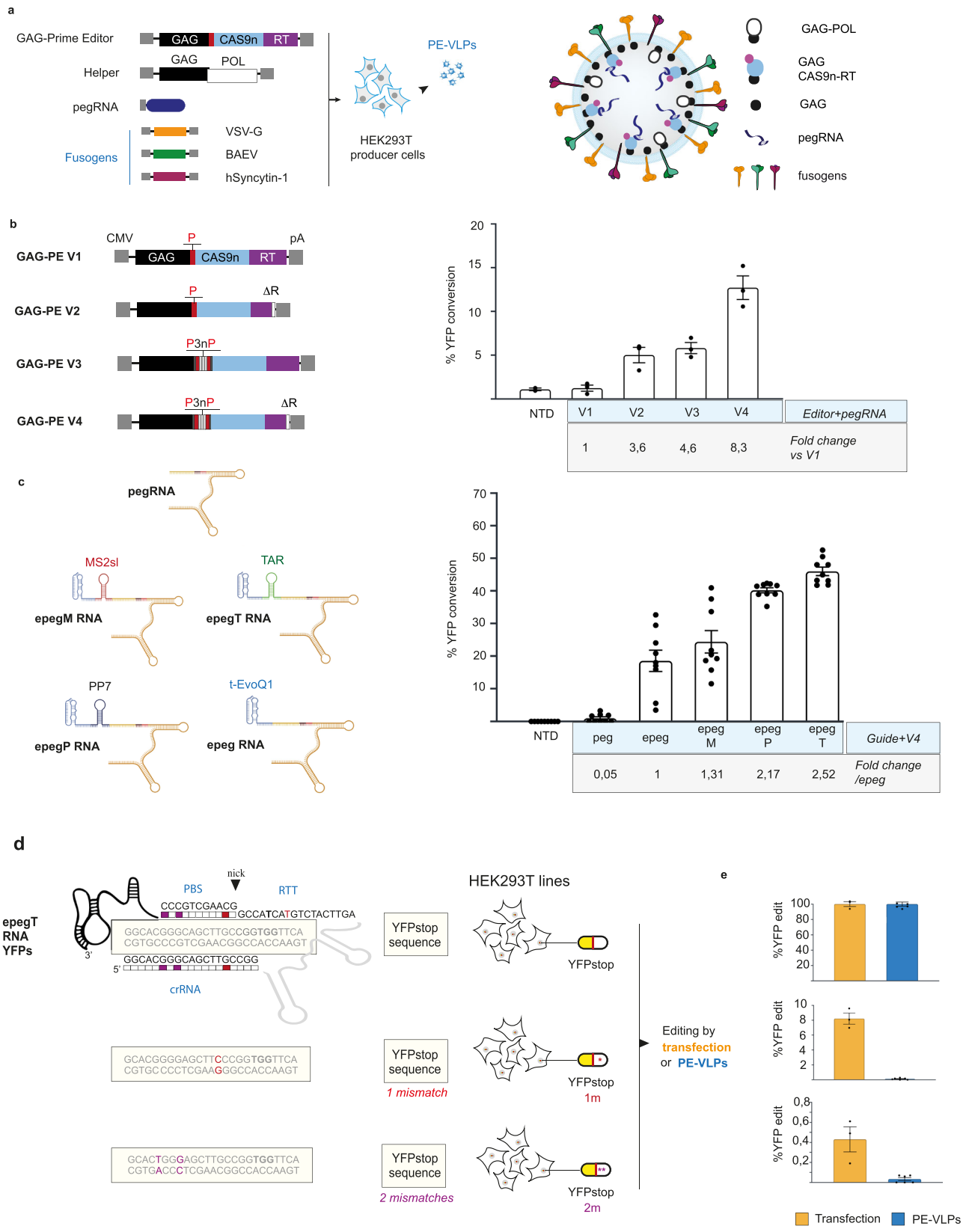

genes) of known pathological variants were shown to possess 4 or more thymines in their sequences thus representing a serious hurdle for an efficient universal PE strategy[33]. In addition, U6 promoters require a G at the +1 position for maximal efficiency which further constrains the design of pegRNAs[34]. Therefore, we adapted a Pol II promoter expression system to generate epegRNAs, as previously described[33]. Pol II promoters are known for robust expression in HEK293T cells[35] and can be used for the expression of multiple epegRNAs from a single transcriptional unit using the Csy4 endoribonuclease for RNA processing[36]. Accordingly, we inserted the epegRNA coding sequence, flanked by two Csy4 hairpin motifs (Csy4HP), within the intron of beta globin (Supplementary Fig. 2a) and

Fig. 1 | Molecular engineering of a PE-VLP system. a Constructs involved for PE VLP production (left) and scheme of PE-VLP particles (right). **b** Evolutions of GAG-PE constructs (left) and efficiencies of VLPs produced with GAG-PE V1-V4 and a pegRNA (right). The protease site of MLV (P) and three fused Nuclear Export Signal of HIV-1 (3n) are indicated. ($n = 3$). **c** Structure of (e)pegRNAs targeting YFPs (left). The trimmed-EvopreQ1 structure (t-EvoQ1), MS2sl, TAR and PP7 hairpins are indicated. Created in BioRender. Ohlmann, T. (2024) https://BioRender.com/g43z718. (right) Relative performances of epegRNAs packaged within V4 PE-VLPs ($n = 9$). **d** Principle of the fidelity assay: HEK293T cells were modified by lentiviral transduction to carry a YFP stop cassette or cassettes harboring one or two mismatches relative to the epegT sequence. Sequences of YFPs variants are given with mismatched positions (red for 1 mismatch, purple for 2 mismatches) **e** Measurement of YFP conversion in cells edited by transfection (orange bars) or by PE-VLPs (blue bars). ($n = 3$). Data represent means of transduction in reporter cells +/− S.E.M. NTD: non-transduced conditions. For panels **b c** and **e**, *n* corresponds to independent transduction assays (biological replicates). Source data are provided as a Source Data file. Graphs were Created in BioRender. Ohlmann, T. (2024) https://BioRender.com/s01x964.

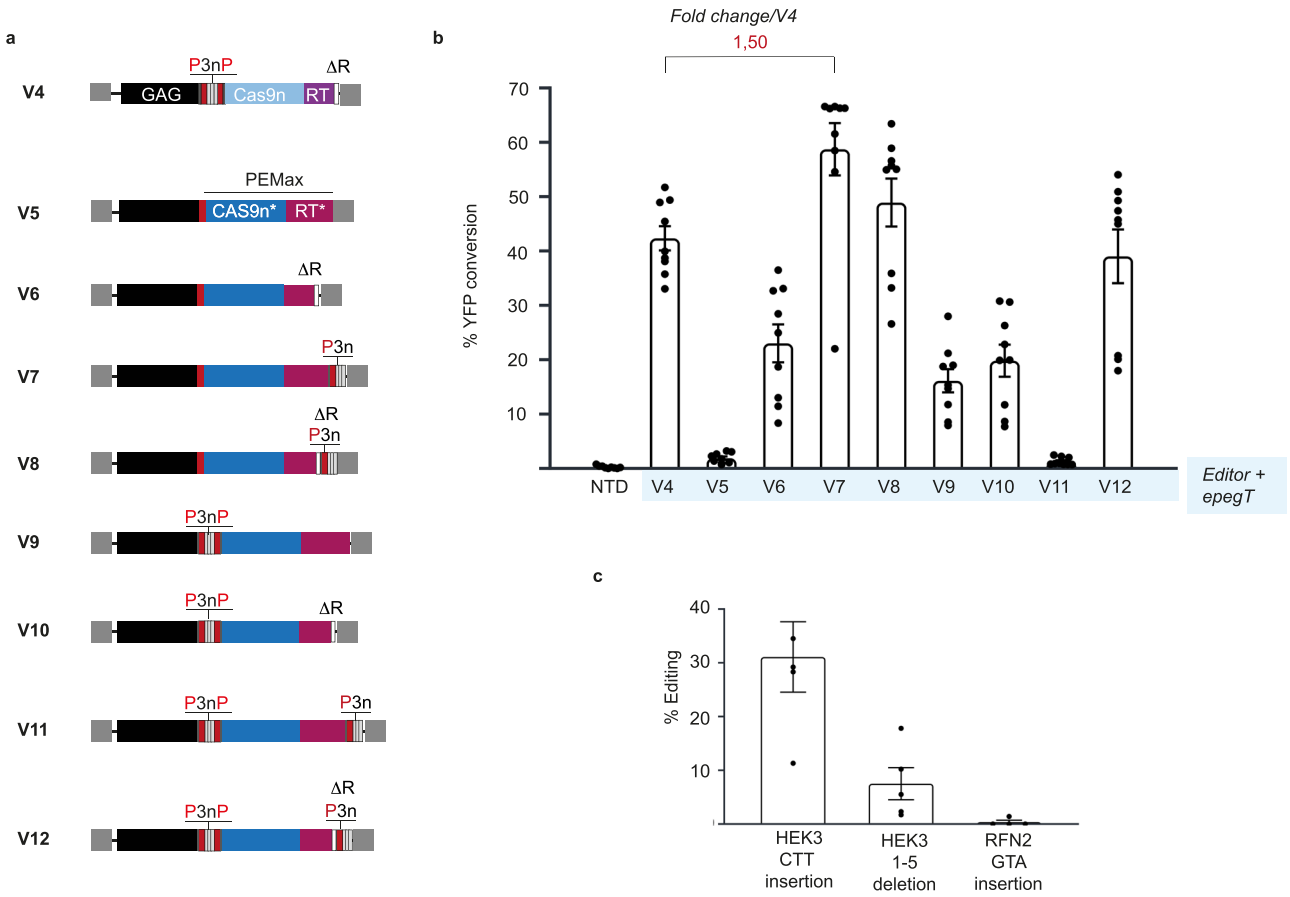

Fig. 2 | Optimization of PE-VLPs performances using the PEmax evolution. a Constructs encoding optimized editors (Cas9n*-RT*: PE Max) fused to GAG. Protease site (P in red) and Nuclear Export Signals from HIV-1 (3n) are indicated. **b** Compared efficiencies of V4-V12 PE-VLPs in transduced SWYS cells. NTD stands for non-transduced condition ($n = 6$). **c** Edition of endogenous locus by PE-VLPs in HEK293T cells ($n = 5$). Data show means +/− SEM. For panels **b** and **c**, n represent independent transduction assays (biological replicates). Source data are provided as a Source Data file. Graphs were Created in BioRender. Ohlmann, T. (2024) https://BioRender.com/s01x964.

defined this design as an 'intronic' pegRNA (ipegRNA). Co-expression of the Csy4 endoribonuclease in producer cells ensures the excision of the ipegRNA with a Csy4HP at its 3' extremity, while an inactive Csy4-mutant[37] failed to process it properly.

Using this approach, we produced three guide RNAs: ipegRNA, ipegTRNA (with TAR RNA) or iepegTRNA (with TAR RNA and trimmed EvopreQ1) (Fig. 3a). These ipegRNAs were then used in PE-VLPs to transduce SWYS cells (Fig. 3b). Our results indicate that the efficiency of the PE-VLP system depends on the presence of the enzymatically active Csy4 protein and that the TAR-containing ipegRNA (ipegTRNA) achieved the highest editing efficiency at 78%. Additionally, the presence of Csy4HP alone (ipegRNA) was sufficient for robust editing even without the trimmed EvoPreQ1 motif. Thus, we assume that the Csy4-HP enhances RNA-stabilization and thus PE efficiency, as previously described[38]. Moreover, this result suggests that the Csy4HP can substitute for trimmed EvoPreQ1, given that iepegTRNA was less efficient than ipegTRNA.

Finally, combining the GAG-PE optimal editor (design V7) with the ipegTRNA in the Pol II expression system further enhanced gene editing efficiency in SWYS-reporter cells, achieving unprecedented performance (Fig. 3c). Specifically, we reached a 91% YFPs conversion rate, comparable to the efficiency obtained by DNA transfection with PE2.

With the development of the Pol II/Csy4 system, we revisited the editing of the *HEK3* (Supplementary Fig. 3) and *RNF2* endogenous loci. We show that both V4 and V7/ipegTRNA edited *HEK3* efficiently with only a moderate increase in efficiency between the two versions (42 % for V4 versus 56 % for V7) (Fig. 3d, left panel). However, using the optimal editor V7 combined with Pol II expressed ipegTRNA targeting *RNF2* resulted in a significant editing increase (6,5 % for V7 versus 2.5 %

https://doi.org/10.1038/s41467-024-55604-0

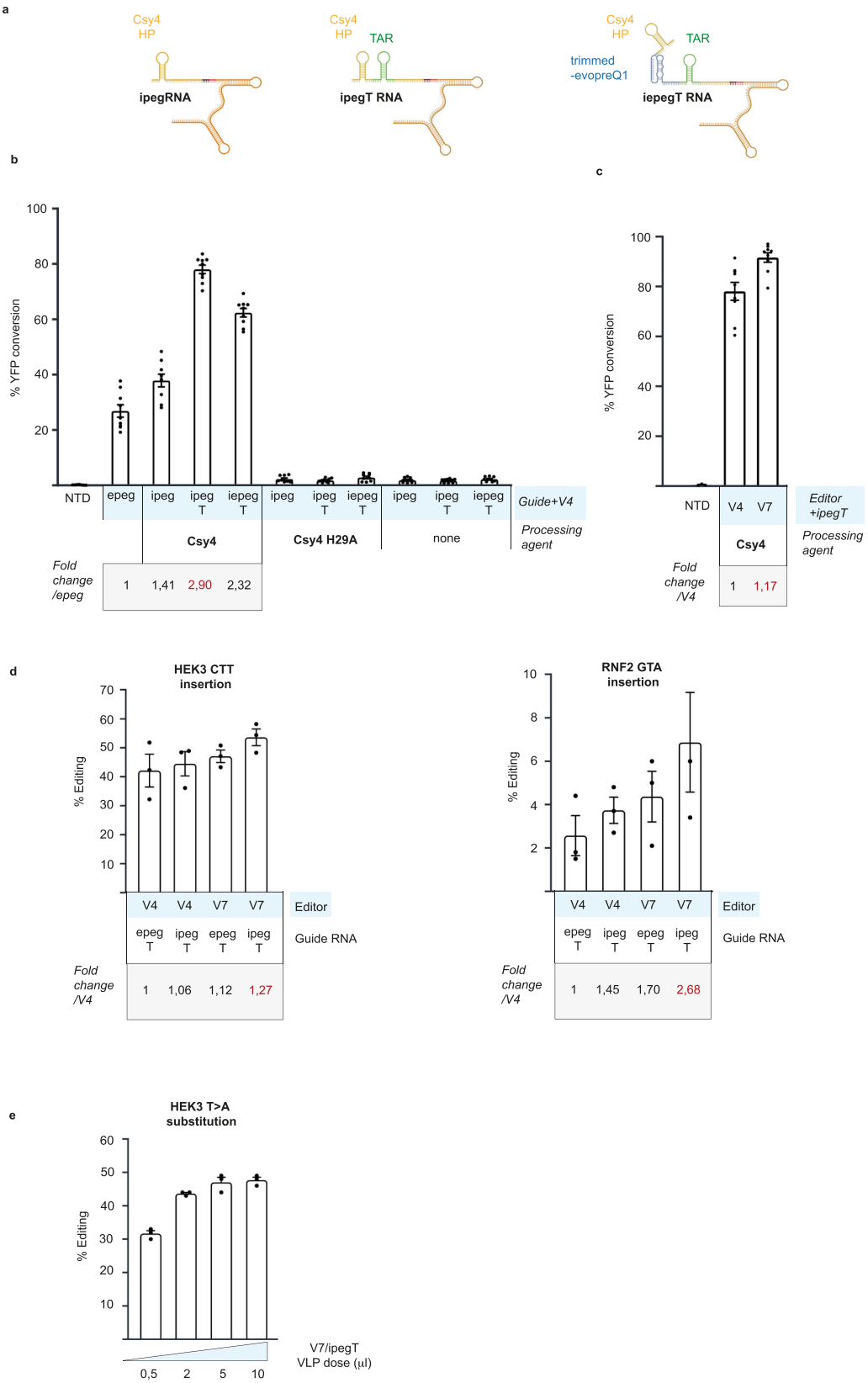

Fig. 3 | Expression of pegRNA with a POL II-promoter enhances prime editing delivery. a Structure of post-splicing ipegRNA and epegRNA. Created in BioRender. Ohlmann, T. (2024) https://BioRender.com/g43z718. **b** Efficacy of PE measured in SWYS cells transduced with GAG-PEV4-VLPs produced from cells expressing intronic-pegRNAs. Production was performed with addition of the Csy4 protein or its non-cleaving mutant Csy4H29A. ($n = 9$) **c** Comparison of GAG-PEV4 and GAG-PE-V7 for the production of ipeg-loaded VLPs. ($n = 9$). **d** Impact of ipegRNA on VLP-efficiencies on endogenous loci (HEK3 CTT insertion) or (RNF2 GTA insertion) ($n = 3$). **e** dose response of PE-VLP-efficiencies (HEK3 T > A substitution) in HEK293t cells ($n = 3$). For all panels, bars represent means +/- SEM and n independent transduction assays (Biological replicates). Source data are provided as a Source Data file. Graphs were Created in BioRender. Ohlmann, T. (2024) https://BioRender.com/s01x964.

for V4) (Fig. 3d right panel). This indicates that the GAG-PEV7/ipegTRNA combination is particularly relevant for suboptimal pegRNAs designs or less-permissive loci.

Multiplexing guide RNAs within PE-VLPs

As previously shown, editing efficiency can be significantly enhanced by using an additional ngRNA to nick the unedited strand[1]. We applied this PE3 strategy by generating PE-VLPs that co-package a ngRNA expressed by a Pol III system together with the ipegTRNA to edit both the endogenous *HEK3* and *RNF2* loci (Supplementary Fig. 4a). Testing various ipegRNA/ngRNA ratios for both targets resulted in moderate improvement of editing efficiency at the *HEK3* (62 % versus 68 % with the ngRNA at a 9:1 ratio) but not at the *RNF2* locus. To improve editing at this particular locus, we attempted to express the intronic ngRNA (ingRNA) on the same construct as ipegRNA, both of which can be released in concert by Csy4 processing[38]. Results (Supplementary Fig. 4b) indicate that the duplex encoding the ipegRNA/ingRNA was highly beneficial to PE-VLP efficacy, with an editing efficiency raised by 1,7-Fold to reach 20% of GTA insertion. This option may increase the efficacy of VLPs engineered with the PE3 system in recalcitrant loci.

Since both ipegRNA and ngRNA compete to complex with Cas9n in particles, we envision that while PE3-VLPs can be engineered, their efficiency will heavily depend on the selected pegRNA/ngRNAs pair, the relative efficiencies of both RNAs and the chosen option to encode them.

Beyond encapsidation of a ngRNA, packaging multiple RNAs by a single VLP preparation could enable co-editing of several genes and the implementation of evolved PE machineries like twin-PE[8] and Bi-PE[39]. To assess the capability of PE-VLPs to package multiple pegRNAs, we produced particles loaded with up to three different ipegTRNAs targeting YFPs, *HEK3* and *RNF2*. Then, we measured editing efficiencies in transduced SWYS cells (Supplementary Fig. 4c). We identified an optimal ipegTRNA ratio (45% *RNF2* / 45% *HEK3* / 10% YFPs) achieving approximately 5% editing at *RNF2*, ~45% at *HEK3* and ~46% at YFPs within the total cell population.

Subsequently, we isolated single cells edited at the YFP locus and derived several sub-clonal populations. Once expanded, we monitored editing events at the *HEK3* and *RNF2* loci by PCR. Amongst YFP-selected clones, 96 % were edited for *HEK3* (blue and violet classes) suggesting that nearly all cells edited at the YFP locus were also edited at the *HEK3* locus. Most importantly, when we looked at clones edited both at the *HEK3* and *RNF2* loci, we found a 46 % of cells were edited at the RNF2 locus (violet class). It is noteworthy that, 100% of these *RNF2*-positive clones were also edited at the *HEK3* locus. These results suggest that co-editing can serve as a basis to target, select and enrich editing at challenging loci.

Prime editing of primary cells, hiPSCs and their derivative hiPSCs-HSC

We next evaluated the capacity of PE-VLPs to edit primary cells for potential therapeutic applications. Primary myoblasts, as muscle precursors, are particularly promising targets for genetic correction strategies. Notably, finely designed PE strategies have been shown to mediate exon-skipping and restore dystrophin expression in edited Myoblasts[40]. For this assay, two waves of PE-VLPS were administrated at 24 h intervals and editing efficiencies were evaluated in proliferating myoblasts or in edited myoblasts differentiated into myotubes (Fig. 4a). Editing efficiency at the *HEK3* locus reached 25% in proliferating myoblasts and maintained a high level in differentiated myotubes (16%), indicating that the PE-VLP treatment did not impair the differentiation process.

To further investigate, we evaluated the capacity of VLPs to edit pluripotent cells such as hiPSCs, which proliferate and can differentiate into various tissue types depending on the treatment conditions[41]. Moreover, hiPSCs are extensively used in disease model development, drug screening assays, and hold significant potential for autologous cell therapy. Safe, accurate and efficient use of PE in these valuable cells is considered promising for gene therapy although delivering of the PE system in hiPSCs remains a significant technical challenge.

First, the AG08C5 hiPSCs control line was transduced with the latest version of our PE-VLPs (V7 with ipegTRNAs) (Fig. 4a). To evaluate the impact of the fusogens on attachment and entry into hiPSCs, we tested PE-VLPs produced with VSV-G only which is commonly used by VLP-users, and our formulation combining fusogens (VSV-G + BAEV +Syncytin-1). Normalized particle amount was used based on virometry counting prior to transduction (See methods). Results showed that gene editing efficiency on *HEK3* reached 15% with the combination of the three fusogens compared to 4% with VSV-G alone thus illustrating the added value of multi-envelope VLPs (Fig. 4b). These results were confirmed with commercially purchased hiPSCs (SCTi003-A), which were edited at a rate of 18%. Furthermore, we assessed the dose response of hiPSCs transduced with increasing volumes of PE-VLPs and showed a linear response to reach a plateau at 15 μL of VLPs (Fig. 4c). To confirm editing, we established subclones from transduced AG08C5 hiPSCs and sequenced the edited region. From a bulk population edited with a suboptimal dose of VLPs (8% of editing), we isolated 24 clones and two them showed editing efficiencies of ~48% (heterozygous) and 99% (homozygous) (Fig. 4d), thus demonstrating that PE-VLPs can edit hIPSCs edited on both alleles. As generating pathological cell types is a significant application of hiPSCs, we tested the ability of the bulk-edited hiPSCs to support cell differentiation, particularly into neural lineage. Edited hiPSCs, with 5% gene editing efficiency were exposed to exogenous stimuli to induce morphogenesis into spheroidal neural progenitor structures within nine days (Supplementary Fig. 5a). Subsequent disaggregation of these progenitors revealed expression of the Olig2 lineage marker and the Tubulin beta-3 protein (Supplementary Fig. 5b). At day 14, nascent motoneurons were morphologically evaluated and immunostained for Islet1 and Tubulin beta-3, confirming the ability of edited hiPSCs to differentiate into specific tissue. Furthermore, we found that the insertion of the CTT triplet was maintained at relatively high levels in progenitor cells (3.9%) and also in young motoneurons (3.6%), compared with the initial bulk population at 5% (Supplementary Fig. 5c). We next investigate whether PE-VLPs could target hiPSCs differentiated into Hematopoietic Stem Cells (HSCs) which are a gold-standards for studying developmental hematopoiesis. AG08C5 hiPSC-HSCs were transduced with PE-VLPs (V7) with an efficiency of 26 % when administered 9 days after the start of differentiation. This efficiency decreased to ~10% when cells were transduced three days later (12 days) (Fig. 4e), suggesting a complex balance between cell differentiation stage and editing efficacy, as previously suggested[42]. Differentiation may also impact the expression of surface markers or cell factors essential for VLP-uptake or their intracellular processing.

Discussion

We describe the development of Nanoscribes virus-like particles that integrate and deliver Prime Editing components in a broad variety of cells. While this work was in progress, Dr Liu and colleagues published a study reporting the engineering of a PE-VLP system, which also fused PEmax with GAG from MLV and modified the structure of the pegRNA[43]. As such, our data complement and implement the work of Liu and colleagues by adding some important features, such as the combination of three fusogens, a TAR-containing epegRNA, a Pol II/Csy4 expression system and the validation of multiplex editing. We noted that the editing efficiencies achieved with our technology rival the values described by this previous report in a similar transduction assay (Fig. 3.e). In addition, we noted that the gag-PE $_{DL}$ editor construct described by An and colleagues behaves much like our V7 editor in a side-by-side assay, and that PE-VLPs produced with gag-PE $_{DL}$ were

https://doi.org/10.1038/s41467-024-55604-0

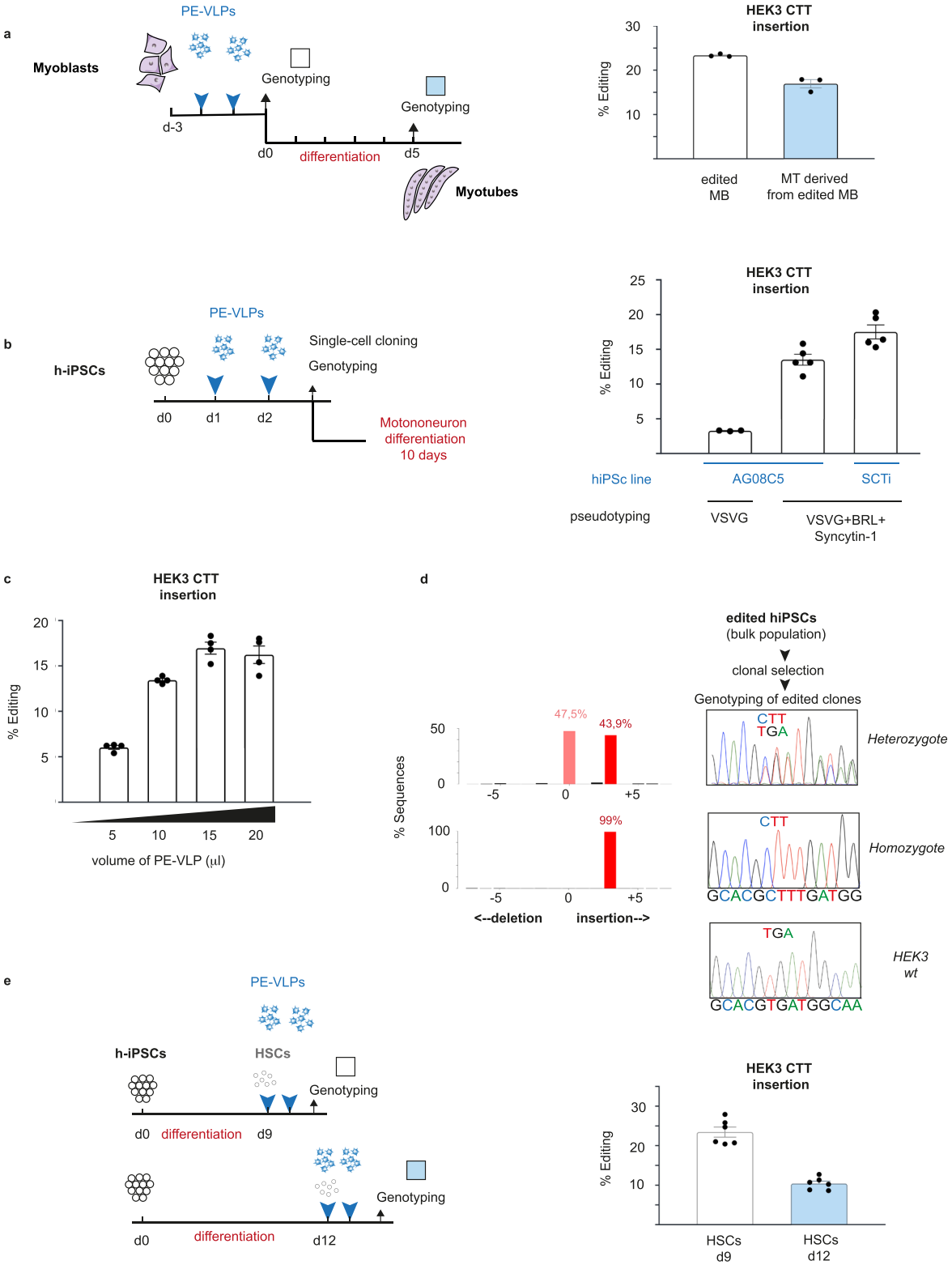

Fig. 4 | Edition of Myoblasts h-IPSCs and h-IPSC-derived hematopoeitic stem cells (HSCs) by PE-VLPs. a Edition of Myoblasts (MB) and myotubes (MT) derived from edited myoblasts by V7/ipegT PE-VLPs. ($n = 3$). **b** Edition of HEK3 in human induced pluripotent stem cells (hiPSCs) by PE-VLPs pseudotyped with VSVG ($n = 3$) or with three envelopes. Types of hiPSC are indicated. STCi stands for SCTi003-A cells ($n = 5$). **c** Dose response of editing efficiencies in hiPSCs transduced by increasing amounts of VLPs ($n = 4$). **d** TIDE analysis of h-IPSC edited clones and corresponding chromatograms. Nucleotides at the site of edition are annoted. Red bars show signals with a P value < 0,005 (two-tailed t-test of the variance–covariance matrix of the standard errors.) **e** Edition of the HEK3 locus in human hematopoeitic stem cells (HSCs) derived from hiPSCs by PE-VLPs ($n = 6$). For **a b** and **e** differentiation/transduction protocol is schematized and days of transduction are depicted by blue arrows representing two administrations of VLPs at 24-hour intervals. Bars represent means +/− SEM and n independent transduction assays (Biological replicates). Source data are provided as a Source Data file. Graphs were Created in BioRender. Ohlmann, T. (2024) https://BioRender.com/s01x964.

significantly more effective when produced with three fusogens, the pseudotyping option we implemented in this report (Supplementary Fig. 6). Importantly, we demonstrate the potential of our VLPs on human cells of great therapeutic interest, such as primary myoblasts and hiPSCs.

Based on our precedent study[29], we first fused the GAG polyprotein to the prime editor 2 (PE2)[8] or to the Prime Editor max construct[2]. To benchmark the PE-VLP system, an exogenous YFP-stop cassette was used to assess the capacity of PE-VLP to efficiently induce prime editing in target cells. Subsequently, we improved the efficiency of VLPs by modifying the structure of the GAG-PE, by the addition of nuclear export signals, proteolytic signals and by deleting the RNaseH domain of the reverse transcriptase. In the meantime, we further stabilized the epegRNA structure by adding a MS2, PP7 or the HIV-1 TAR stem loops before the EvoPreQ1 pseudoknot at the 3′ end of the epegRNA. Generally, inserting the TAR stem-loop significantly improved Prime Editing with VLPs suggesting that this structure might alleviate some bottleneck effects that were less obvious if Prime-Editing effectors were administrated by transfection. This could be explained by the higher thermodynamic stability of the TAR stem loop[44] or by its interaction and binding to cellular factors[45], all these parameters that may be even more critical in a VLP production context. Finally, we developed a Pol II expression system for the pegRNAs compatible with the production of VLPs. The latter system relies on the use of the Csy4 endonuclease to process an intronic pegRNA (ipegRNA). These RNAs are tagged in 3′ by a Csy4 hairpin that enhanced editing compared to our previously optimized Pol III epegTRNA. This may be due to the presence of the Csy4HP at their 3′ end, which can be bound by the Csy4 protein forming a more stable protein-RNA complex. Such a hypothesis is supported by the fact that in class I type I-F Cas operons, Cas6 mediates crRNA maturation and processing by binding and staying on the Csy-4 HP[46]. Also, the release of csy4-dependent ipegRNAs occurs in the cytoplasm, which might increase the pool of ipegRNAs available for packaging into VLPs compared with a Pol III system.

We have engineered an optimal VLP design in which V7 is associated with ipegTRNA encoded by a pol II-construct. Performances of the V7 version was verified for the editing of YFPs (Fig.3c), as well as for an endogenous HEK3 locus (Supplementary Fig. 3). The optimized VLP system allowed to insert an edit at the *HEK3* and *RNF2* loci in HEK293T cells up to 60% and 14% respectively, with a significant improvement for RNF2 (20%) with the addition of a PE3-ingRNA (Supplementary Fig. 4b). This suggests that Nanoscribes can effectively edit human cell lines endogenously with efficiency depending on the loci and the edit types selected. For the *HEK3* locus the maximal efficiency attained (68% for CTT insertion) was higher than what could be reached with AAV transduction[12] and close to levels achieved by transfection[1]. To impose the T > A substitution in the same locus, a low-dose of Nanoscribes achieved 48% of editing in HEK293T (Fig3.e).

PE-VLPs can be used to deliver multiple guide RNAs such as ngRNAs for the PE3 system or multiple ipegTRNAs which could mediate prime editing at each targeted locus. This opens the way for the multiplexing of pegRNA in a single encoding construct[36], or permits to set up elaborated prime editing evolutions including twin-PE[8], Bi-PE[39] or selection procedures involving several peg/gRNAs[47–49].

Due to the absence of double-strand DNA breaks (DSB) and thanks to the molecular checkpoints provided by the pegRNA on its DNA target, PE, especially the PE2 method, is significantly more accurate than the classical CRISPR-Cas9 system[4]. To verify this notion for PE-VLPs, we have developed a complementary mismatch fidelity assay in which the YFPs target locus was degenerated in one or two positions. We verified that the use of PE-VLPs exhibited a much higher fidelity than DNA transfection (Fig. 1e). This is an important consideration for the use of PE in research laboratories, and even more essential for its application in gene therapy.

Finally, we have evaluated the efficacy of Nanoscribes on cells of clinical relevance, namely myoblasts, hiPSCs and hiPSC-derived HSCs, which serve as pivotal models for gene therapy and regenerative medicine. The use of PE in these cells holds significant promises due to their susceptibility to DSB, which may lead to chromosomal rearrangements and activation of apoptosis via the p53 pathways[50,28]. Consequently, the conventional CRISPR/Cas9 editing strategy is severely constrained in these contexts.

Thus, we have assessed Nanoscribes on primary myoblasts, hiPSC as well as hiPSC-derived HSCs. After successful transduction with PE-VLPs, we achieved editing efficiencies ranging from 15% hiPSCs to 25% (hiPSC-derived HSC), akin to the performance of classical PE2 approach as previously described[7,51]. Importantly, we also demonstrated the efficient generation of clonal hiPS cell lines, with 2 out of 24 clones exhibiting pure editing hiPSCs populations (Fig. 4d).

Finally, our findings also underscored the enhanced efficacy of multi-enveloped PE-VLPs resulting in an editing efficiency of nearly 20% in hiPSCs, outperforming VLPs bearing only the VSV-G envelope (Fig. 4b). Although not strictly essential for VLP production, fusogen multiplexing can also reduce the dose of particles required for efficient transduction compared with single-envelope VLPs (Supplementary Fig. 6b). Antibody-dependent pseudotyping systems[22,23] or natural fusogens[21] could be implemented in the future to limit the immunogenicity of PE-VLPs or modulate their tropism for specific targets.

In summary, we have engineered optimized-VLPs that allow the delivery of the PE in the form of a RNP complex warranting both safety and target specificity. Nanoscribes can perform single or multiplexed editing with an efficiency comparable to DNA/mRNA/RNP transfection. As such, they represent a particularly relevant and promising tool for the treatment of human therapeutic cells.

Methods

Molecular constructs

GAG-PE V1 was constructed by inserting into the PE2 construct[1] a PCR-amplified fragment corresponding to a CMV-fMLVGAG-PS (Protease site) cassette between SnaBI and NotI. Primers were F: 5′-CTTGGCAGTACATCTACGTATTAGTCATCG-3′ and R: 5′- gatatcgcgg ccgcccaccggtaggtgtgagggctggatacagggaac-3′ and template was BIC-CAS9 (Addgene #119942). GAG-PE derivatives were next constructed by conventional cloning. Plasmids coding for PE2 (#132775), PEmax (#174820) and Csy4 (55196) were obtained from Addgene. Sequences of pegRNA used in this study are provided in Supplementary Data file 1.

Cultured cells

Primary human myoblasts were obtained from the Centre de Biotechnologie Cellulaire, (Groupement Hospitalier Est, Bron, France). hIPSC cells SCTi were commercially purchased (Stem cells catalog # 200–0510). hIPSC cells AG0 were etablished at the PGNM lab by reprogrammation of human foreskin fibroblasts and characterized by Stem Genomics (STR analysis, iCS-digital™ PSC) and by Karyotyping and pluripotent tests (3-layers differentiation): https://hpscreg.eu/cell-line/PGNMi001-A. The HEK293T-LentiX cell-line used for VLP production and transduction tests was purchased from Clontech (Catalog number:632180). A549 and U2OS cell lines were obtained from ATCC (number CCL-185 and HTB-96 respectively).

Production of PE-VLPs

To produce PE-VLPs; 4,5 × 10^6 HEK293T cells have been seeded in a 10cm-diameter dish 24 h prior to transfection with 10µg of a plasmid mixture including GAG-PE, pegRNA, a plasmid encoding GAG-POL from Friend-murine leukemia virus and fusogens. Transfection was performed using JetOptimus (Polyplus) according to the manufacturer instructions. Optimized proportions of this transfection mix are 18 % of GAG-PE, 30% of GAG-POL, 15% of fusogens and 37% of pegRNA, 100% corresponding for total DNA input. For production of mCherry-loaded

particles and Csy4-dependent VLPs, 5% of GAG-mCherry or Csy4-encoding plasmid were added in the transfection mix, respectively, impacting the other plasmids amounts equally. In most experiments the fusogen-mix contains a VSV-G encoding plasmid (5%), a plasmid encoding a truncated R-less version of BAEV exploited in our previous VLP-system (5%), a plasmid encoding human Syncytin-1 (5%). For the production of Csy-4-dependent Nanoscribes in a 10-cm dish, these amounts correspond to 17 µg of GAG-PE V7, 28,5 µg of GAG-POL, 0,5 µg of VSVG, 0,5 µg of BRL, 0,4 µg of Syncytin-1, 0,5 µg of Csy4, and 35 µg of ipegRNA. Large productions were performed in 10-cm dishes (10µg of total transfected DNA) or in 6-w plates for comparative studies (2µg of total DNA).

48 h after transfection the supernatant have been harvested, clarified by centrifugation (400 g, 5 minutes), filtered through a 0,45 µm pore-sized filter and concentrated by ultracentrifugation (1h15, 7 °C and 35000 g). Subsequently, pellets were resuspended in a volume corresponding of 1/100 of the supernatant volume. For a 10 ml supernatant volume, VLPs were classically resuspended in 100 µl of 0,2 µm-filtered PBS which is referred as a 100x concentration. For VLPs dedicated to precursor cells, particles were concentrated through a 10%-sucrose cushion.

P30 dosages of different PE-VLP preparations were performed using the Quicktiter MuLV Core antigen ELISA KIT VPK-156 (Cell Biolabs) and measured concentrations between 1,54-2,07 ng of p30 per ml, which is equivalent to a mean of 1,57x10e12 virions/µl. For most experiments, three independent VLP batches were systematically produced, each of them being tested in three independent transduction assays.

Characterization of the SWYS cell line and implementation of a standard-transduction assay

A *YFP* transgene interrupted by a stop codon was inserted in a lentiviral construct encoding also the puromycine-resistance gene (Supplementary Fig. 1A). Lentiviral particles produced using this construct (SWYS) were next used to transduce HEK293T at low multiplicity of infection (0,1) to minimize the risk of a double integration event, and cells were diluted and cultivated with puromycine before the picking of single-cell derived clones. After several passages, a PE-reacting clone was amplified and frozen. We verified that this reporter cell line responded linearly to increasing amounts of PE-VLPs (Supplementary Fig. 1e), with the apparition of a progressive flattening of the curve for editing values above 60%. We measured a close correlation between the percentage of YFP signal in edited cells and the percentage of effective genome editing measured by Sanger sequencing.

To measure efficiencies of editing mediated by PE-VLPs a standard transduction procedure was classically followed: 1×10^4 SWYS cells were plated in a 96-well plate and transduced 24 h latter by 5µl of concentrated PE-VLPs. Edited fluorescent cells were analyzed 72 h later by flow-cytometry. For the transduction of endogenous targets in cell lines, volumes of VLPs were raised up to 10 µl.

Analysis of triplet insertion in the *HEK3* and *RNF2* loci

Genomic DNA from treated Cells were extracted at least 48 h after transduction with a commercial kit (Rapid Lyse Macherey Nagel) and the edited region of the *HEK3* locus was next amplified by PCR using primers

F: 5′- TCTTGTAGCTACGCCTGTGATGGGC-3′ and
R: 5′- TCTGACCACTGCGATATGACCACCC-3′.
PCR conditions were 5 min 94 °C, 3 cycles (94 °C 30 sec, 64 °C 30 sec, 72 °C 30 sec) followed by 25 cycles (94 °C 30 sec, 57 °C 30 sec, 72 °C 30 sec).
For the *RNF2* locus, PCR amplification was performed with the following primers:
F: 5′- GCACTAATTTCATTCATGAGGGTGG-3′ and
R: 5′- CAATGTCTGTAAAGTCCATGGTTGG-3′.
PCR conditions were 5 min 94 °C, 3 cycles (94 °C 30 sec, 56°C 30 sec, 72 °C 30 sec), 2 cycles (94 °C 30 sec, 51°C 30 sec, 72 °C 30 sec) followed by 25 cycles (94 °C 30 sec, 47 °C 30 sec, 72 °C 30 sec).
30-80 ng of genomic DNA were classically used for template with the GOTAQ polymerase (Promega).

Amplicons were next purified by magnetic beads (NGS-size purification kit Macherey Nagel) and eluted in 30ul before Sanger Sequencing (MicroSynth). Primers for sequencing was: 5′- TGAATCAGTGCTGGAGAATGGG-3′ for HEK2 and 5′- GCACTAATTTCATTCATGAGGGTGG-3′ for *RNF2*. Finally, chromatograms were analyzed with TIDE[52] with following parameters: Lb70, DW 298-428 IS7. Signals with a *P*-value below 0,001 were considered, except for Fig. 4d where this limit was 0,005.

Co-edited clone analysis

For production, 4.10^6 HEK293T cells were seeded 24 h prior to transfection as described in "Production of PE-VLPs" however, an exception was made in the number of iPegTRNA used for transfection. Indeed, one, two or three iPegTRNA were used with the following ratios: 1:0, 3:1, 1:1, 1:3, 0:1 or 5:5:1, 5:1:5, 1:5:5, 4:1:1, 4:4:1,1:4:1 (iPegTRNA *HEK3* + 1 CTT: iPegTRNA *RNF2* + 1GTA or iPegTRNA *HEK3* + 1CTT: iPegTRNA *RNF2* + 1GTA: iPegTRNA YFPs). Next, 10^4 SWYS cells were seeded and transduced with 10 µL of each PE-VLPs then genetic modifications were assessed either as described in "Analysis of triplet insertion in the *HEK3* and *RNF2* loci" for genetic modifications or as described in "Characterization of the SWYS cell line and implementation of a standard-transduction assay" for fluorescence quantifications. Subsequently, 2.10^3 SWIS cells edited by the PE-VLP with an iPegTRNA ratio of 5:5:1 was seeded on a 100 mm cell culture plate and clonal isolation of YFP-positive clones was performed. For analysis, only clones with a percentage of YFP fluorescence superior or equal to 90% were kept for PCR-based detection of the *HEK3* and *RNF2* loci modifications. Finally, cells were sorted by class based on the presence or absence of the modifications on their genomic DNA.

hiPSCs culture and transduction with PE-VLPs

Human iPSCs were maintained on GelTrex (Thermo Fisher Scientific) in iPS-Brew XF medium (Miltenyi Biotec) or in mTeSR™ (STEMCELL Technologies), respectively, for AG08C5 (#PGNMi001-A on hPSCreg) and SCTi003-A (STEMCELL Technologies) hiPSC lines. Cells are passaged with Versene for routine passaging, or with Enzyme Express TripLE (Thermo Fisher Scientific) for single celling, at a density of 10^4 cells/cm^2 every 3 to 4 days and cultured at 37°C, 5% CO2. After passaging, Y-27632 is added for 24 h, followed by daily medium changes. For the transduction assay with PE-VLPs, hiPSCs are seeded at 20,000 cells per well in 24-well plates. The next day, they are transduced for 48 hours with 2 doses of PE-VLPs at 24-hour intervals in 200 µL of hiPSC medium without Y-27632 for 4 hours, after which 500 µL of fresh hiPSC medium is added.

hiPSC-derived HSCs and transduction with PE-VLPs

AG08C5 iPSCs (#PGNMi001-A on hPSCreg site) were differentiated for 9 or 12 days using the STEMdiff™ Hematopoietic Kit (#05310, STEMCELL Technologies, Inc.). On day 9 or 12 of differentiation, the cells were split with TripLE, seeded at a density of 2.10^4 cells/cm^2 in 24-well plates and transduced for 48 hours with 2 doses of PE-VLPs at 24-hour intervals in 300 uL of Medium B of the STEMdiff™ Hematopoietic kit.

hiPSC-derived motor neuron (MNs) precursors

Human iPSC-derived MNs were generated as previously described[53,54]. AG08C5 iPSCs were dissociated with TrypLE and 3×10^5 cells were seeded in 6-well plates treated with anti-adhesion solution (StemCell Technologies) to form embryoid bodies (EBs). On day 9, EBs of neural progenitors were dissociated in single cells with TripLE and plated on

poly-L-ornithine (Sigma)-Laminin (Sigma)-coated 24-well plates at 40,000 cells/cm^2. The differentiation protocol was continued until day 14.

Myoblasts culture, differentiation into myotubes, and transduction with PE-VLPs

Primary human myoblasts were obtained from the Centre de Biotechnologie Cellulaire, (Groupement Hospitalier Est, Bron, France). Cells were then expended in proliferating KMEM medium (1 volume of M199, 4 volumes of Dulbecco's modified Eagle's medium (DMEM), 20% fetal bovine serum (v/v), 25 µg/mL Fetuin, 0.5 ng/mL β-FGF, 5 ng/mL EGF, 5 µg/mL Insulin from Gibco BRL). Differentiation of the human myoblasts into myotubes was carried out in DMEM + insulin (10 µg/mL) for 5 days.

For the transduction assay on myoblasts, cells were plated at a density of 2.10^4 cells/cm^2 in 24-well plates and transduced the day after for 48 hours with 2 doses of PE-VLPs at 24-hour intervals in 200 µL of myoblast medium for 4 hours, after which 500 µL of fresh medium is added. Some treated myoblasts were induced to differentiate into a differentiated medium for 5 days.

Flow-virometry characterization of particles

Flow-virometry quantifications were performed using a MacsQuant VYB device (Miltenyi) calibrated using calibration beads of known sizes (Megamix). To unambiguously distinguish viral-like particles from the electronic noise, particles were internally stained by the incorporation of GAG-mCherry or externally labelled by a VSV-antibody coupled with FITC (Abcam), or double stained by both stainings. Settings of the device were set to allow the detection of 500 nm beads in the same window as the 100 nm beads. Counting of particles was performed considering events strictly between these two borders. To minimize coincidence and abort rate, particles were diluted by at least 100-fold before acquisition at low speed. Particle counts were systematically repeated for several dilution conditions: linearly-correlated counts were considered. Using the flow rate of the device (25 µl in 1 minute) and the time of acquisition, we were able to measure the physical titer of particle batches. We noted that our approach was relevant and reproducible on the VYB-MacsQuant instrument and was confirmed using the Aurora spectral cytometer (Cytek) equipped with a violet SSC laser at the Flow-Virometry Core, SFR LYON BIOSCIENCES.

Staining particles with VSV-G antibody

Concentrated particles were classically diluted 10-fold in filtered PBS and stained using a FITC-coupled antibody detecting VSV-G (Abcam ab3863) diluted at 1/100. After 3 hours at 25 °C in the dark, the stained solution (10µl) was diluted 10 times by addition of 90 µl of cold-filtered-PBS before acquisition. Depending on the initial concentration, stained particles were further diluted 10-fold higher prior to FACS-acquisition in PBS.

Staining of motoneurons

Cells were incubated 10 min at room temperature in 3,7% formaldehyde/PBS, washed three times with PBS and incubated in blocking buffer (PBS + BSA4% +glycine 0,1 M +triton 0,3%) for 1 hour at room temperature. Diluted primary antibody (diluted in blocking buffer) were next incubated 1 hour at room temperature, before three PBS washes and incubation with fluorophore-conjugated secondary antibodies and Dapi for 1 hour at room temperature, diluted in blocking buffer. After three washes with PBS, cells were analysed.

Antibody dilutions were: Islet1 R&D Systems AF1837 dilution factor 1/500, Olig2 Millipore AB9610, dilution factor 1/200, β3-tubuline Biolegend 801202, dilution factor 1/1000, Dapi Sigma D9542 dilution factor 1/2500.

Statistics and Reproducibility

No statistical method was used to predetermine sample size and no data were excluded from the analyses. The experiments were not randomized and the investigators were not blinded to allocation during experiments and outcome assessment. For TIDE analysis, results with a *P*-values below 0,001 (0,005 for Fig. 4d) were considered (two-tailed *t*-test of the variance–covariance matrix of the standard errors).

Reporting summary

Further information on research design is available in the Nature Portfolio Reporting Summary linked to this article.

Data availability

Source data are provided with this paper.

References

1. Anzalone, A. V. et al. Search-and-replace genome editing without double-strand breaks or donor DNA. *Nature* **576**, 149–157 (2019).
2. Chen, P. J. et al. Enhanced prime editing systems by manipulating cellular determinants of editing outcomes. *Cell* **184**, 5635–5652.e29 (2021).
3. Gao, R. et al. Genomic and Transcriptomic Analyses of Prime Editing Guide RNA-Independent Off-Target Effects by Prime Editors. *CRISPR J.* **5**, 276–293 (2022).
4. Kim, D. Y., Moon, S. B., Ko, J.-H., Kim, Y.-S. & Kim, D. Unbiased investigation of specificities of prime editing systems in human cells. *Nucleic Acids Res.* **48**, 10576–10589 (2020).
5. Nelson, J. W. et al. Engineered pegRNAs improve prime editing efficiency. *Nat. Biotechnol.* **40**, 402–410 (2022).
6. Hwang, H.-Y. et al. Precise editing of pathogenic nucleotide repeat expansions in iPSCs using paired prime editor. *Nucleic Acids Res* gkae310 (2024) https://doi.org/10.1093/nar/gkae310.
7. Li, H. et al. Highly efficient generation of isogenic pluripotent stem cell models using prime editing. *Elife* **11**, e79208 (2022).
8. Anzalone, A. V. et al. Programmable deletion, replacement, integration and inversion of large DNA sequences with twin prime editing. *Nat. Biotechnol.* **40**, 731–740 (2022).
9. Wolff, J. H. & Mikkelsen, J. G. Prime editing in hematopoietic stem cells-From ex vivo to in vivo CRISPR-based treatment of blood disorders. *Front Genome Ed.* **5**, 1148650 (2023).
10. Haldrup, J. et al. Engineered lentivirus-derived nanoparticles (LVNPs) for delivery of CRISPR/Cas ribonucleoprotein complexes supporting base editing, prime editing and in vivo gene modification. *Nucleic Acids Res* **51**, 10059–10074 (2023).
11. Dong, J. Y., Fan, P. D. & Frizzell, R. A. Quantitative analysis of the packaging capacity of recombinant adeno-associated virus. *Hum. Gene Ther.* **7**, 2101–2112 (1996).
12. Gao, Z. et al. A truncated reverse transcriptase enhances prime editing by split AAV vectors. *Mol. Ther.* **30**, 2942–2951 (2022).
13. Böck, D. et al. In vivo prime editing of a metabolic liver disease in mice. *Sci. Transl. Med* **14**, eabl9238 (2022).
14. Davis, J. R. et al. Efficient prime editing in mouse brain, liver and heart with dual AAVs. *Nat. Biotechnol.* **42**, 253–264 (2024).
15. Thomas, C. E., Ehrhardt, A. & Kay, M. A. Progress and problems with the use of viral vectors for gene therapy. *Nat. Rev. Genet* **4**, 346–358 (2003).
16. Wang, D., Tai, P. W. L. & Gao, G. Adeno-associated virus vector as a platform for gene therapy delivery. *Nat. Rev. Drug Discov.* **18**, 358–378 (2019).
17. Cai, Y., Bak, R. O. & Mikkelsen, J. G. Targeted genome editing by lentiviral protein transduction of zinc-finger and TAL-effector nucleases. *Elife* **3**, e01911 (2014).
18. Choi, J. G. et al. Lentivirus pre-packed with Cas9 protein for safer gene editing. *Gene Ther.* **23**, 627–633 (2016).

19. Lyu, P., Javidi-Parsijani, P., Atala, A. & Lu, B. Delivering Cas9/sgRNA ribonucleoprotein (RNP) by lentiviral capsid-based bionanoparticles for efficient 'hit-and-run' genome editing. *Nucleic Acids Res* **47**, e99 (2019).
20. Bender, R. R. et al. Receptor-Targeted Nipah Virus Glycoproteins Improve Cell-Type Selective Gene Delivery and Reveal a Preference for Membrane-Proximal Cell Attachment. *PLoS Pathog.* **12**, e1005641 (2016).
21. Hindi, S. M. et al. Enveloped viruses pseudotyped with mammalian myogenic cell fusogens target skeletal muscle for gene delivery. *Cell* **186**, 2062–2077.e17 (2023).
22. Strebinger, D. et al. Cell type-specific delivery by modular envelope design. *Nat. Commun.* **14**, 5141 (2023).
23. Hamilton, J. R. et al. In vivo human T cell engineering with enveloped delivery vehicles. *Nat Biotechnol* (2024) https://doi.org/10.1038/s41587-023-02085-z.
24. Schauber-Plewa, C., Simmons, A., Tuerk, M. J., Pacheco, C. D. & Veres, G. Complement regulatory proteins are incorporated into lentiviral vectors and protect particles against complement inactivation. *Gene Ther.* **12**, 238–245 (2005).
25. Milani, M. et al. Phagocytosis-shielded lentiviral vectors improve liver gene therapy in nonhuman primates. *Sci. Transl. Med* **11**, eaav7325 (2019).
26. Raguram, A., Banskota, S. & Liu, D. R. Therapeutic in vivo delivery of gene editing agents. *Cell* **185**, 2806–2827 (2022).
27. Liang, S.-Q. et al. Genome-wide profiling of prime editor off-target sites in vitro and in vivo using PE-tag. *Nat. Methods* **20**, 898–907 (2023).
28. Haapaniemi, E., Botla, S., Schmierer, B. & Taipale, J. CRISPR-Cas9 genome editing induces a p53-mediated DNA damage response. *Nat. Med* **24**, 927–930 (2018).
29. Mangeot, P. E. et al. Genome editing in primary cells and in vivo using viral-derived Nanoblades loaded with Cas9-sgRNA ribonucleoproteins. *Nat. Commun.* **10**, 45 (2019).
30. Bernardi, A. & Spahr, P. F. Nucleotide sequence at the binding site for coat protein on RNA of bacteriophage R17. *Proc. Natl Acad. Sci. USA* **69**, 3033–3037 (1972).
31. Lim, F. & Peabody, D. S. RNA recognition site of PP7 coat protein. *Nucleic Acids Res* **30**, 4138–4144 (2002).
32. Zhang, J. et al. HIV-1 TAR RNA enhances the interaction between Tat and cyclin T1. *J. Biol. Chem.* **275**, 34314–34319 (2000).
33. Huang, S. et al. Broadening prime editing toolkits using RNA-Pol-II-driven engineered pegRNA. *Mol. Ther.* **30**, 2923–2932 (2022).
34. Ma, H. et al. Pol III Promoters to Express Small RNAs: Delineation of Transcription Initiation. *Mol. Ther. Nucleic Acids* **3**, e161 (2014).
35. Moens, U. et al. Simian virus 40 large T-antigen, but not small T-antigen, trans-activates the human cytomegalovirus major immediate early promoter. *Virus Genes* **23**, 215–226 (2001).
36. Nissim, L., Perli, S. D., Fridkin, A., Perez-Pinera, P. & Lu, T. K. Multiplexed and programmable regulation of gene networks with an integrated RNA and CRISPR/Cas toolkit in human cells. *Mol. Cell* **54**, 698–710 (2014).
37. Haurwitz, R. E., Jinek, M., Wiedenheft, B., Zhou, K. & Doudna, J. A. Sequence- and structure-specific RNA processing by a CRISPR endonuclease. *Science* **329**, 1355–1358 (2010).
38. Liu, Y. et al. Enhancing prime editing by Csy4-mediated processing of pegRNA. *Cell Res* **31**, 1134–1136 (2021).
39. Tao, R. et al. Bi-PE: bi-directional priming improves CRISPR/Cas9 prime editing in mammalian cells. *Nucleic Acids Res* **50**, 6423–6434 (2022).
40. Happi Mbakam, C. et al. Prime editing strategies to mediate exon skipping in DMD gene. *Front Med (Lausanne)* **10**, 1128557 (2023).
41. Liu, G., David, B. T., Trawczynski, M. & Fessler, R. G. Advances in Pluripotent Stem Cells: History, Mechanisms, Technologies, and Applications. *Stem Cell Rev. Rep.* **16**, 3–32 (2020).
42. Wang, Q., Capelletti, S., Liu, J., Janssen, J. M. & Gonçalves, M. A. F. V. Selection-free precise gene repair using high-capacity adenovector delivery of advanced prime editing systems rescues dystrophin synthesis in DMD muscle cells. *Nucleic Acids Res.* gkae057 (2024) https://doi.org/10.1093/nar/gkae057.
43. An, M. et al. Engineered virus-like particles for transient delivery of prime editor ribonucleoprotein complexes in vivo. *Nat. Biotechnol.* (2024) https://doi.org/10.1038/s41587-023-02078-y.
44. Lorenz, R. et al. ViennaRNA Package 2.0. *Algorithms Mol. Biol.* **6**, 26 (2011).
45. Kong, W. et al. Nucleolar protein NOP2/NSUN1 suppresses HIV-1 transcription and promotes viral latency by competing with Tat for TAR binding and methylation. *PLoS Pathog.* **16**, e1008430 (2020).
46. Sternberg, S. H., Haurwitz, R. E. & Doudna, J. A. Mechanism of substrate selection by a highly specific CRISPR endoribonuclease. *RNA* **18**, 661–672 (2012).
47. Levesque, S. et al. Marker-free co-selection for successive rounds of prime editing in human cells. *Nat. Commun.* **13**, 5909 (2022).
48. Schene, I. F. et al. Mutation-specific reporter for optimization and enrichment of prime editing. *Nat. Commun.* **13**, 1028 (2022).
49. Frisch, C. et al. PINE-TREE enables highly efficient genetic modification of human cell lines. *Mol. Ther. Nucleic Acids* **33**, 483–492 (2023).
50. Ihry, R. J. et al. p53 inhibits CRISPR-Cas9 engineering in human pluripotent stem cells. *Nat. Med* **24**, 939–946 (2018).
51. Habib, O., Habib, G., Hwang, G.-H. & Bae, S. Comprehensive analysis of prime editing outcomes in human embryonic stem cells. *Nucleic Acids Res* **50**, 1187–1197 (2022).
52. Brinkman, E. K., Chen, T., Amendola, M. & van Steensel, B. Easy quantitative assessment of genome editing by sequence trace decomposition. *Nucleic Acids Res* **42**, e168 (2014).
53. Maury, Y. et al. Combinatorial analysis of developmental cues efficiently converts human pluripotent stem cells into multiple neuronal subtypes. *Nat. Biotechnol.* **33**, 89–96 (2015).
54. Jacquier, A. et al. Severe congenital myasthenic syndromes caused by agrin mutations affecting secretion by motoneurons. *Acta Neuropathol.* **144**, 707–731 (2022).

Acknowledgements

Authors acknowledge the Cytometry Core Facilities of SFR Biosciences (Université Claude Bernard Lyon 1, CNRS UAR3444, Inserm US8, ENS de Lyon) and the PGNM IPS-Core facility headed by A.J. and V.R. This work was supported by a grant from Agence Nationale de Recherche sur le Sida et les hépatites virales (T.O. grant number ANRS0516), by AFM Téléthon through the MyoNeurALP strategic grant and the MyoPharm Agrin grant (V.R., J.C., L.C., L.S., A.J). T.H. is a recipient of a PhD fellowship from the french ministère de la recherche et de l'enseignement supérieur.

Author contributions

P.E.M. and T.H. conceived the study, T.H., P.E.M., V.R., J.C. conceived planned and carried out most of the experiments with contributions of L.C. and M.R.T.O., L.S., A.J. contributed to the interpretation of the results. P.E.M., T.O., T.H. wrote the manuscript in consultation with V.R. All authors provided critical feedback.

Competing interests

T.H., P.E.M. and T.O. are inventors of two patents owned by Inserm Transfert EP N° EP24305987.0 and EP 24305808.8 protecting the molecular designs of constructs of the final Nanoscribes system. Patent application numbers are pending. The remaining authors declare no competing interests.

Additional information

Supplementary information The online version contains supplementary material available at https://doi.org/10.1038/s41467-024-55604-0.

Correspondence and requests for materials should be addressed to Théophile Ohlmann or Philippe Emmanuel Mangeot.

Peer review information *Nature Communications* thanks Baisong Lu and the other, anonymous, reviewer(s) for their contribution to the peer review of this work. A peer review file is available.